An Adaptive Operational Strategy for Providing Frequency Containment Reserve in Wind Turbines

Nezmin Kayedpour[a], Jeroen D. M. De Kooning[a,b], Arash E. Samani[a,b], Lieven Vandevelde[a,b], Guillaume Crevecoeur[a,b]

[a]*Department of Electromechanical, Systems and Metal Engineering, Ghent University, Technologiepark-Zwijnaarde 131, 9052 Ghent, Belgium*
[b]*FlandersMake@UGent—core lab MIRO, 9052 Ghent, Belgium*

Abstract

As conventional power plants based on fossil fuel are being phased out, it is desirable that wind energy conversion systems participate more in delivering grid balancing services, such as Frequency Containment Reserve (FCR). Therefore, an adaptive operational strategy is needed to optimally control active power and accommodate the power reserve margin under stochastic wind conditions and grid frequency uncertainties. This study investigates an end-to-end operational approach, from estimating an appropriate deloading margin to the real-time computation of generator torque and pitch control set-points based on the grid frequency considering the fixed and percentage reserve methods. The Group Method of Data Handling algorithm predicts grid frequency time series. A real-time lookup table dynamically adjusts the power reserve and adapts the deloading rotor speed-power curve based on a short-term estimation of the grid frequency. An adaptive gain scheduled fuzzy-PI pitch and torque controls are implemented to enhance the dynamic response and establish a smooth provision of FCR in partial-load and full-load operation. A series of simulations on the 5MW-NREL offshore model in the presence of turbulent winds assess the performance of the suggested scheme. The simulation results demonstrate the effectiveness of the proposed control system in varying wind and grid frequency conditions.

Keywords: , Wind turbine, Grid frequency, Frequency containment reserve, Adaptive fuzzy-PI controller, Structural loads

1. Introduction

Wind energy conversion systems are among the most promising technologies that support a low-carbon energy system. The installed wind power capacity has grown substantially during the last couple of decades [1]. This capacity has been increased up to 837 GW by the end of 2022 [2]. Approximately 12.4% of the new capacity is installed in the last year, only 1.8% lower than 2020's record year [2]. Offshore wind energy is expected to supply around 30% of the electricity demand by 2050, representing at least 50% of the total energy mix [3]. However, extensive penetration of wind sources into the power grid seriously affects the power system's frequency stability. The primary reason for the blackout events on 9 August 2019 in the UK was the sudden decline in frequency beyond the regulation capability of system inertia [4]. The unpredictability, stochastic, and highly fluctuating nature of wind energy with less directly coupled inertia are the main reasons that result in the grid's inertia degradation consequently [5]. Therefore, system operators require to involve wind energy sources in providing ancillary services. These ancillary products can be in the form of hierarchical frequency control, including Frequency Containment Reserve (FCR), automatic Frequency Restoration Reserve (aFRR), and manual Frequency Restoration Reserve (mFRR) [6, 7]. Many Wind Turbine (WT) manufacturers have already rolled out enhanced control systems that include the functionality of inertial and frequency response [8]. However, developing methodologies to improve the capability of providing active power control and frequency regulation is an active field of research, both in academia and industry [9, 10, 11, 12]. This article mainly focuses on the FCR provision, in which an operating reserve is required for constant containment of frequency deviations from the nominal value to maintain the power balance in the aggregate synchronous grid.

Numerous investigations have been performed to focus on the possibility of WTs participating in frequency containment reserve through active power control. In order to improve the frequency regulation capability, an available power reserve is needed for actively responding to grid frequency changes. Therefore, the WT's power output must be deloaded by specific percentages [13]. However, the deloading strategies are not yet perfectly developed for WTs in different wind speed zones and operating conditions. In [14], the operating wind speed is divided into low, medium, and high zones, and a deloading strategy for WTs is developed to perform differentiated reserve capacity allocation. The power reserve in different operating conditions can be obtained by derating/deloading the WT through the pitch controller (above-rated wind speed), lowering the torque, and operating on a suboptimal tip-speed ratio (below-rated wind speed). The realizations of deloading operation in DFIG-Based WTs, which can be done via rotor over speeding control (converter controlled) and pitch angle control (actuator controlled), are discussed in [15]. Recently, the active power control provision for Variable-Speed WTs has been studied in [9], improving the primary frequency contribution considering wind fluctuations

and power smoothing. Moreover, adaptive frequency control strategies in isolated power [16] and in a grid-connected system under power imbalance conditions [17] are studied.

Furthermore, advanced control approaches such as multiple-input multiple-output Linear Quadratic Gaussian (LQG) controller and Model Predictive controller are employed to improve the frequency regulation in [18, 19]. Fuzzy Inference System (FIS)-based methods can also offer adaptive control performance, especially when an operation strategy should be applied in varying operating regions. In [20], a hybrid control method based on a Fuzzy-Proportional Integral Derivative (Fuzzy-PID) control strategy is applied for a pitch system of an offshore WT with a direct-driven Permanent Magnet Synchronous Generator (PMSG). In [21], a novel Fuzzy-Proportional-Integral (Fuzzy-PI) pitch control is proposed to improve the power adjustment, resulting in decreased fatigue loads of the tower base and the blade root by up to 21.53% in normal turbulent wind conditions and by up to 18.14% in extremely turbulent wind conditions. Recently, a fuzzy logic-based linear quadratic regulator (LQRF) control algorithm for a variable-speed variable-pitch WT was introduced in [22], which can reduce the tower vibrations by up to 12.50% and improve the power regulation by 38.93% depending on the operating region. In [23], the fuzzy logic pitch controller performance is optimized by applying a genetic algorithm. Additionally, [24] adjusts the deloading level of the WT generations in a real-time framework. This adjustment is according to the wind speed, regardless of the grid frequency behavior, and the activation of power reserve, which depend on a complex cooperation between renewables, thermal power units, and demand response.

The mentioned studies neglect the adaptiveness of the power reserve and adjustment of the same unit deloading operation regarding grid frequency stochasticity, which must be considered to enhance the flexibility of the FCR provision. Lack of focus can be witnessed in the literature regarding adaptive operation of WT considering varying power reserve for different frequency scenarios. This approach can potentially lead to optimal deloading operation and maximizing wind power production. This study proposes a dynamic deloading strategy to operate WTs wwith a real-time and adaptive margin estimation according to the grid frequency variations through different wind speed zones. The suggested deloading framework is investigated for fixed and percentage reserve strategies. In the fixed reserve mode, also known as delta mode, a fixed amount of reserve is set, while in percentage reserve mode, the reserve margin corresponds to a percentage of the available wind power [8]. The reserve margin should be adequately estimated to avoid an over-deloading performance. The deloading margin can be set to the output level of WTs in a dynamic way adapting to the time-varying stochastic wind speed and grid frequency. It prevails over the dynamic trade-off concern of frequency regulation and output maximization of wind power. To do so, real-time power system frequency information that shows the balance between generation and demand should be estimated using a historical time-series data set to reflect the frequency variations and features, such as Nadir. An accurate system frequency observation is required to estimate the adequate power reserve, which will likely be activated in the next window of the prediction horizon.

This study proposes an end-to-end operation strategy that enables a wind turbine coupled with a Permanent Magnet Synchronous Generator (PMSG) to provide FCR by first analyzing the power system frequency using the Group Method of Data Handling (GMDH) as a data-driven time-series prediction approach. Secondly, estimating the power reserve that can be adapted to the variations of grid frequency. Thirdly, estimating the generator torque and pitch control set-points by considering a real-time lookup table that adaptively justifies the rotor speed and electrical power operating curve considering varying wind speeds. Fourthly, employing advanced control approaches to constantly operate the wind turbine with adaptive scheduled gains. Since the wind turbine needs to operate under varying conditions and activate different power reserves, fuzzy-PI pitch and torque controllers are designed to achieve an adaptive gain scheduling performance. Finally, comprehensive simulations are studied for extensive operating conditions under various scenarios of wind and frequency to evaluate the performance of the proposed end-to-end operation strategy.

This study is arranged as follows: Section II presents the 5MW WT dynamic and baseline control designs. The proposed adaptive reserve strategy and deloading methods are discussed in section III. Section IV introduces the adaptive fuzzy-PI pitch and speed control design. The controller performance assessment and clarification are given in section V. Discussion and conclusions are presented in section VI.

2. Wind turbine baseline control system

This work studies a 5MW NREL offshore WT model, which has a conventional variable-speed, variable blade-pitch-to-feather configuration. The baseline controller, consisting of a gain-scheduled PI, has been implemented according to the control design section introduced in [25]. The baseline control system relies on a generator-torque controller and a full-span rotor-collective blade-pitch controller. The two essential control systems are designed to work independently in all operating regions. As shown in Figure1, the operating mode depends on the wind speed and can be divided into four regions. In the first two regions where the wind speed is below the rated value, the pitch angle is kept in an optimal position, and the generator-torque controller aims to maximize power capture.

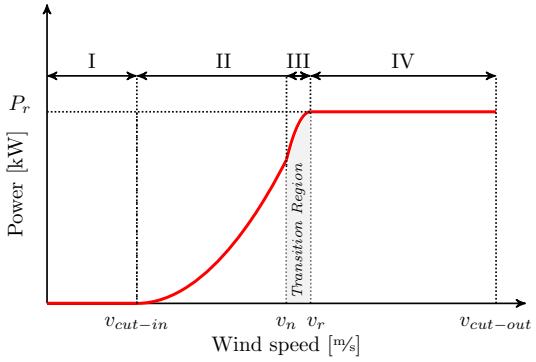

Figure 1: Wind turbine operating regions.

This is known as the Maximum Power Point Tracking (MPPT) mode. The third region, transition zone, can be considered an extension of the second. In this region, the primary objective is to regulate generator speed at rated power using a pitch control system. The blade-pitch controller aims to regulate generator speed in the fourth region, where the wind speed is above the rated value. In general, the nonlinear relationship between aerodynamic power P_a and wind speed v can be formulated as follows:

$$P_a = \frac{1}{2}\rho R^2 \pi v^3 C_p(\lambda, \theta) \tag{1}$$

$$\lambda = \frac{\omega_r R}{v} \tag{2}$$

where C_p is the power coefficient, ρ is the air density, R is the blade length and θ is the pitch angle of the blade. λ is the tip-speed ratio, which is a function of wind and rotational speed, v, and ω_r, respectively. The mechanical torque can be formulated as follows:

$$T_m = \frac{1}{2\lambda}\rho R^3 \pi v^2 C_p(\lambda, \theta) \tag{3}$$

The mechanical equation of motion is given by:

$$T_m - T_g = J\frac{\mathrm{d}\omega_r}{\mathrm{d}t} + F\omega_r \tag{4}$$

where, J is the moment of inertia, F is the viscous friction coefficient, and T_g is the electromagnetic torque from the generator. FAST implements Blade Element Momentum (BEM) and simulates the nonlinear aerodynamics. It also determines structural response to wind-inflow conditions in time, which is advantageous for developing control designs and analysis [26, 27].

In this article, the direct-drive PMSG is also modeled with an equivalent scheme in the rotating reference frame, as suggested in [28]. The machine's realistic dynamics and losses, including machine inductances, the armature reaction effect, stator winding copper losses, and iron core losses, are considered and included in the efficiency curve. The dynamic equivalent model of the PMSG can be formulated in the q,d rotating reference frame:

$$V_d = R_s I_d + L_d\frac{\mathrm{d}I_d}{\mathrm{d}t} - N_P\omega_r L_q I_q \tag{5}$$

$$V_q = R_s I_q + L_q\frac{dI_q}{dt} + N_P\omega_r(L_d I_d + \Phi_m) \tag{6}$$

where, R_s is the stator-winding resistance, L_d and L_q are the d-axis and q-axis stator-inductances, Φ_m is the flux linkage, V_d and I_d are d-axis stator voltage and current, respectively, V_q and I_q are q-axis stator voltage and current, respectively, and N_p is the pole pair number. The generator torque and electrical power can be calculated as follows:

$$T_g = \frac{3}{2}N_p\left[\Phi_m I_q + (L_d - L_q)I_d I_q\right] \tag{7}$$

$$P_e = \frac{3}{2}\left[V_d I_d + V_q I_q\right] \tag{8}$$

The generator control uses field orientation, i.e., the torque is controlled by regulating the q-axis current while maintaining the d-axis current at zero. It is out of scope of the current work to use a full-switching model of the power-electronic converter. Instead, an efficiency curve is obtained from a separate Simulink model to represent its losses realistically. The Simulink model includes conduction and switching losses up to the switching level [29]. No additional control actions, such as startup sequences, shutdown sequences, and safety functions, are considered. The nacelle-yaw control system is not included in the analysis as it is deemed too slow to contribute to FCR activation, as this requires sufficiently fast power control. Figure 2 shows the baseline control system that regulates the rotational speed with an outer control loop based on power and an inner torque control loop. The outer proportional-integral (PI) controller loop is the (slow) power controller giving the reference signal to the (fast) inner control loop, regulating the generator current through control of the active rectifier. A pre-defined lookup table determines the reference signal of the cascaded control system. The lookup table is created from the power-speed curves obtained through simulations. The gain-scheduled PI pitch controller, shown in Figure 2, is developed at each operating point to cope with the nonlinear aerodynamic sensitivity. The blade-pitch sensitivity is calculated for the 5MW NREL turbine model by performing a linearization analysis in FAST [30].

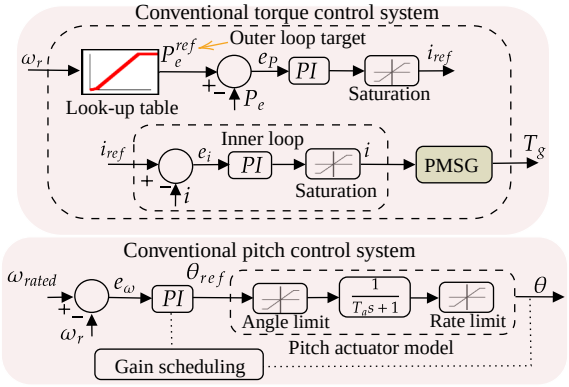

Figure 2: Wind turbine baseline control system.

In this study, the aerodynamic forces on the blades and the tower are obtained from AeroDyn, based on Automated Dynamic Analysis of Mechanical Systems (ADAMS) and integrated in FAST. The land-based version of the NREL 5-MW baseline is employed for offshore floating systems, which incorporates several degrees of freedom (DOF), i.e., two flapwise and one edgewise bending mode DOF for the blades, one variable generator speed DOF, one driveshaft torsional DOF, and two fore-aft and two side-to-side bending mode DOFs for the tower [30].

3. Methodology

In FCR provision in which activating upward and downward products must be supported simultaneously, WTs cannot operate in MPPT mode and must be deloaded. However, since the active power should be regulated proportionally to the frequency changes, the maximum contribution usually will

not be asked to be activated continuously. Therefore, the WT could be only deloaded to satisfy the expected request for the predicted horizon. In this section, a control scheme, shown in Figure 3, is discussed in which a varying reserve margin can be estimated based on the grid frequency prediction. Moreover, a supplementary control structure is also introduced that adaptively copes with the estimated reserve and provides control setpoints to the pitch and torque control systems. Then, an adaptive fuzzy gain scheduling PI is suggested for following the electrical power and rotational speed in all operating regions.

3.1. Reserve margin estimation and Grid frequency prediction

To provide FCR, the measured grid frequency is converted into a frequency response, considering a deadband of 10mHz, through a corresponding change in active power output ΔP, which is proportional to grid frequency deviations Δf ($f_{\text{ref}} = 50\ Hz$) with a droop coefficient D. The promised reserve contribution must be respected once the wind farm decision-maker selects the reserve bids based on probable wind speed scenarios and FCR prices in the day-ahead reserve market. Therefore, the decided droop coefficient D should be maintained for a 200 mHz symmetric product with a frequency deviation of 40.8 to 50.2 Hz under any circumstances. However, the grid frequency distributions for the last five years, shown in Figure 4, indicate the grid frequency varies with less strong deviations (49.94 to 50.06 Hz). Thus, this study suggests an optimal but still conservative approach that considers an adequate reserve margin for the potential activation by adapting the reserve margin β to the lowest expected frequency drop f^{pre}_{e-min} for a short-term prediction horizon. Then, as indicated in Figure 3, the reserve margin will be decided considering f^{pre}_{e-min} and the prediction error E_{pre}.

In this study, a nonlinear regression method is employed as a semi-supervised deep learning tool that automatically self-organizes the predictive distribution of variables. GMDH can drive the best polynomial network structure to accurately reveal the approximated function and predict future values from historical datasets. The GMDH time series prediction considers a general relationship between delayed inputs and output variables in the form of polynomial functions, which is referred to as the Volterra function series or the Kolmogorov–Gabor polynomial function expressed by:

$$y = a_0 + \sum_{i=1}^{m} a_i x_i + \sum_{i=1}^{m}\sum_{j=1}^{m} a_{ij} x_i x_j + \sum_{i=1}^{m}\sum_{i=1}^{m}\sum_{k=1}^{m} a_{ijk} x_i x_j x_k \quad (9)$$

where y is the response variable, x is the vector of lagged time series to be regressed, m is the number of variables, and a_0, a_i, a_{ij} and a_{ijk} are the weighting factors. In this study, the quadratic K-G polynomial is employed in the form of:

$$z = f(x_i, x_j) = b_0 + b_1 x_i + b_2 x_j + b_3 x_j x_i + b_4 x_i^2 + b_5 x_j^2 \quad (10)$$

The GMDH structure can be trained to realize the relationship among the lags with the function f. The proposed stochastic approximation algorithm is developed based on a

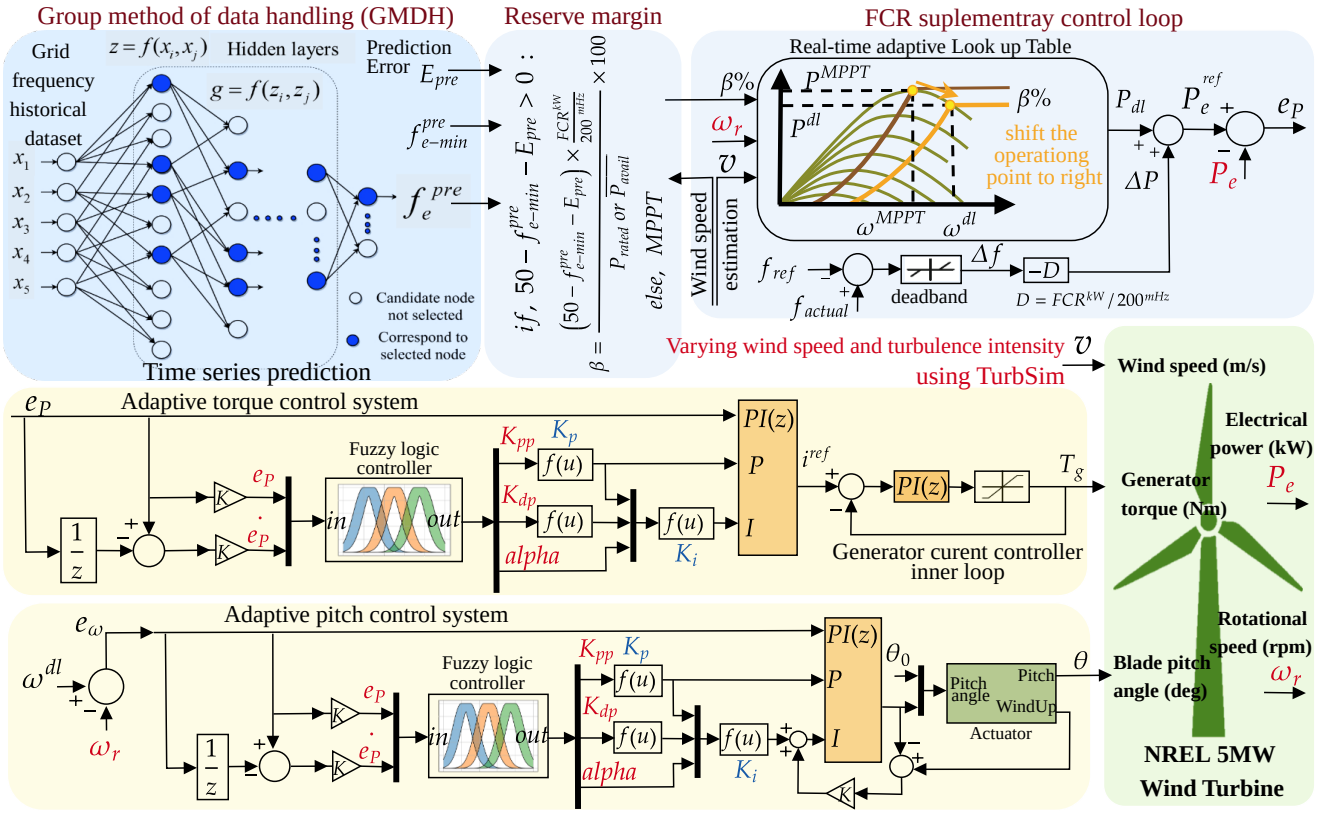

Figure 3: Proposed control architecture and the FCR supplementary control loop.

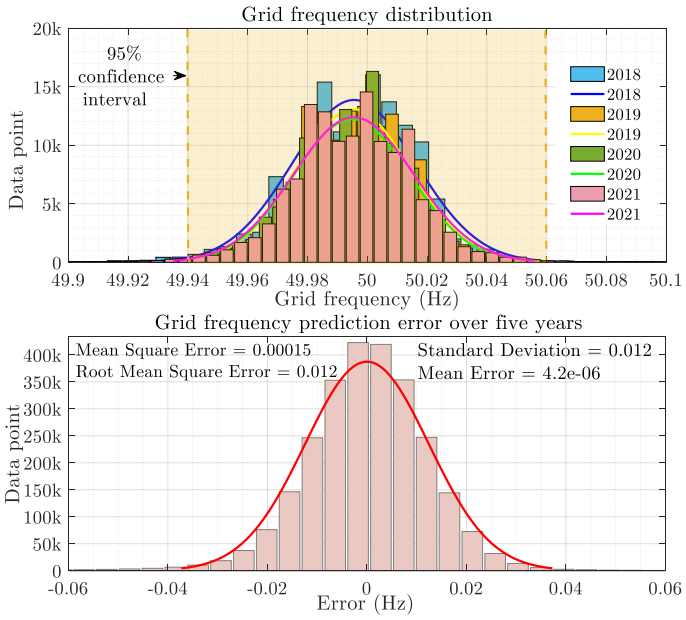

Figure 4: Grid frequency distribution and prediction error.

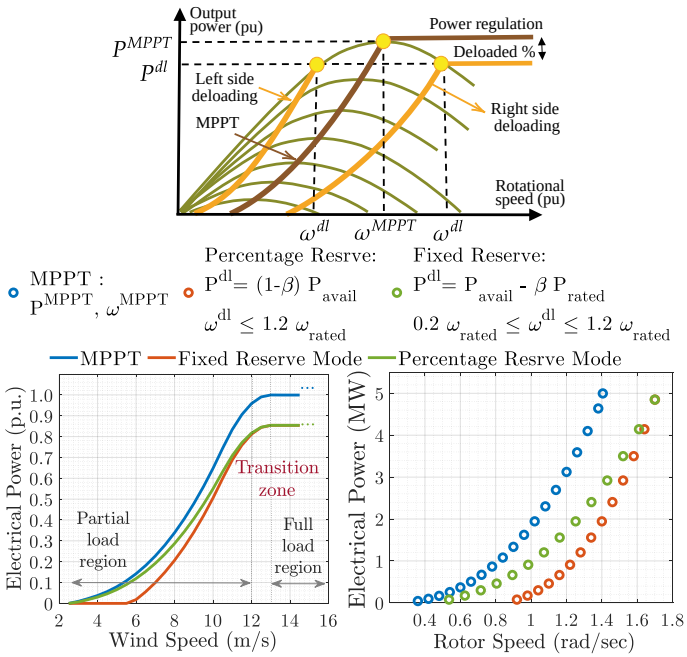

Figure 5: Rotor speed adjustment for WT deloading operation (top), Power curve as a function of wind speed (bottom-left), Calculation of power reference and rotational speed for deloaded operation (bottom-right).

multilayer network using various component subsets of the polynomial function for each layer. In this algorithm, the output obtained from the last layer will be set as a new input variable for the next layer. All possible tries of two independent variables are taken out of a total n inputs to conduct a regression polynomial in the form of (10) in the first layer. Therefore, the minimum activation function is the second-order polynomial, but it can be gradually increased to higher orders to find an architecture with optimal complexity. A threshold restricts the number of solutions using the external criterion to find the fittest structure. The parameters are estimated using the least-squares regression method over five years of the historical data set, i.e., from January 2017 to October 2022, with a 10-second sample time. The prediction horizon is set to 550s with five delayed inputs. The Mean, Root Mean Square Error (RMSE), Mean Square Error (MSE), and Standard Deviation (SD) of the absolute errors are the evaluation metrics used for assessing the results, which are given in Figure 4.

3.2. *Power reserve strategies*

The estimated reserve margin can be achieved through three main deloading strategies introduced in [31], e.g., derating, fixed power reserve, and percentage reserve control modes. The baseline pitch controller is the same for the three deloading types, whereas the generator-torque controller is slightly different. Figure 5 shows a deloaded power curve and the steady-state power capture of each power reserve strategy. The WT is able to satisfy the scheduled FCR at the above-rated wind speed. However, it is required to deload the wind turbines at below-rate wind speeds by shifting the WT operating point towards the left or right of the maximum power point [32]. Thus, a reserve margin will be created by flexibly varying the active power between P^{dl} and P^{MPPT} through changing the rotor speed between ω^{dl} and ω^{MPPT}. This study suggests shifting the operating point to the right to avoid reducing the kinetic energy, which is beneficial for inertial response [33]. Furthermore, an adaptive lookup table is incorporated in the supplementary control loop to capture and reflect the time-varying characteristic of the proposed power reserve. As Figure 3 serves, the deloaded power reference P^{dl} for operating under fixed and percentage reserve modes needs to be estimated by dynamically adjusting the rotational speed. In this method, the reserve margine β represents the portion of P_{rated} (deloading percentage) that specifies the upper limit of generated power in MPPT for the fixed reserve mode. Thus, βP_{rated} represents the saving margin required to be maintained as a constant power reserve. In the percentage reserve mode, $(1-\beta)$ represents the fraction of the available power that can be captured in a way that the rest of capacity βP_{avail} can be maintained as a power reserve which is not constant and fixed but proportionally changes with the available power. Figure 6 shows the power output and the estimated β in both fixed and percentage strategies corresponding to the grid frequency profile by proportionally activating ΔP in a turbulent wind speed. In these simulations, the allowable range of suboptimal rotor speed ω^{dl} corresponds to P^{dl} should be respected, considering the highest permitted limit of rotational speed (determinded by rated rotational speed ω_{rated}). In this case, the suboptimal rotor speed ω^{dl} is limited between $0.2\omega_{rated}$ and $1.2\omega_{rated}$ for the fixed reserve and $\omega^{dl} \leq 1.2\omega_{rated}$ for percentage reserve mode considering maximum 3 MW FCR contribution for 550s.

Figure 6 also indicates that the reserve margin in the percentage reserve strategy tends to increase when wind speed rises. The WT operation is monitored at 8 m/s mean wind

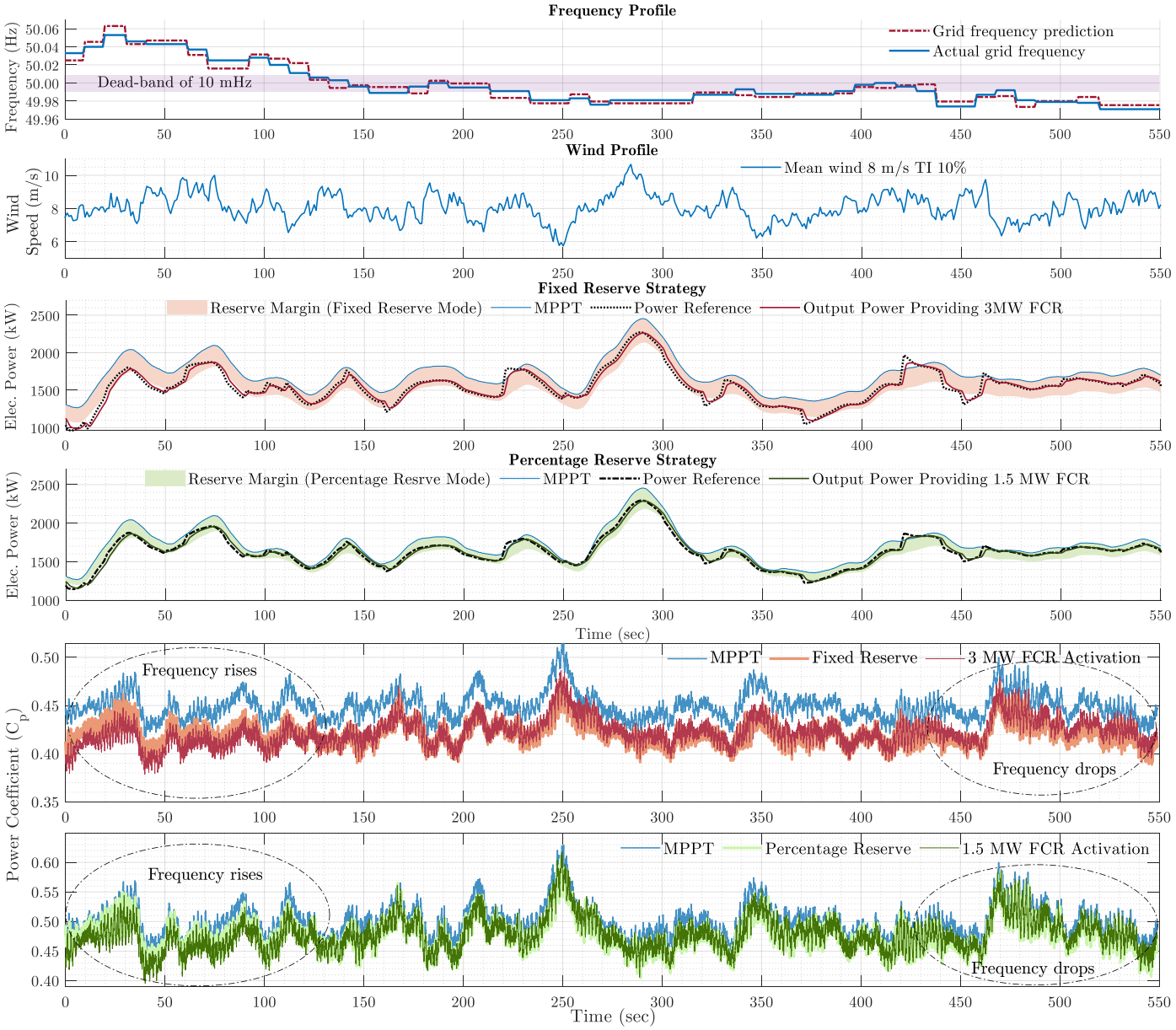

Figure 6: FCR activation under the proposed framework.

speed and 10% turbulence intensity for both strategies. The grid frequency profile used in this study represents frequency rises and drops for 550s with 10s sample rate. The fixed reserve strategy offers FCR twice the amount provided in the percentage reserve mode for the estimated β considering the grid frequency prediction. Although the power reference can be tracked closely in both strategies, the percentage mode can offer less FCR in below-rated wind speeds. The WT power coefficient is also presented in Figure 6 to illustrate the suboptimal operation in different frequency scenarios, i.e., when the frequency drops or rises.

3.3. Adaptive fuzzy-PI control system

PI control is still one of the most successful controllers in industrial processes. However, it typically has poor control performance and stability issues for nonlinear and time-varying systems [34], especially when control actions are needed at different operating points with varying operating conditions and dynamic setpoints. The PI and fuzzy logic algorithm combination offers a promising alternative solution, in which gain parameters are adapted by weighting factors calculated through a fuzzy logic controller [35]. This research studies the performance of fuzzy-PI regulators for pitch and torque control systems in tracking the power reference providing FCR for varying reserve margins and deloading strategies. The derivative action is excluded as it causes an undesired reaction to high-frequency measurement noise.

3.3.1. Fuzzy-PI algorithm

The adaptive gain scheduling fuzzy-PI consists of three components: fuzzification, fuzzy inference system, and defuzzification. The fuzzification generally transforms definite and crisp inputs, errors, and derivative errors, into the form of a fuzzy set and a membership function. As Figure 7.a describes,

any membership corresponds to a fuzzy set through linguistic marks, i.e., NB, NM, NS, Z, PS, PM, and PB, which stands for negative big, negative medium, negative small, zero, positive small, positive medium, and positive big, respectively [36, 37]. The FIS contains the control target derived from expert knowledge and fuzzy-based rules in the form of if-then. The transformation of the control quantity obtained by fuzzy rules into the distinct quantity is called defuzzification. This can be done by means of techniques such as centroid of area, a center of gravity, or the maxima method [38].

The control output and the formulation of fuzzy rules highly depend on the number of fuzzy subsets, such that choosing more fuzzy subsets would improve the control performance [37]. However, selecting a larger number of fuzzy sets would complicate the implementation due to the complex rule-making. In this article, the fuzzy subsets are divided into seven fuzzy subsets based on experience. The input membership functions for (error, derivative error) and the outputs are created with the Gaussian distribution. The singleton parameter α is created using the triangular-shaped membership functions. The membership functions and the corresponding rule surface as the function of inputs and outputs are shown in Figures 7. There are two sets of Gaussian membership functions to fuzzy-PI, which are the crisp values of the error and error derivative. The fuzzy rules are designed to decide the output value for a given case of error and change in error.

3.3.2. *Adaptive fuzzy-PI pitch and generator-torque control design*

Typically, the PI gains should be set to enhance the system's response speed and improve response accuracy. However, an excessive proportional parameter causes overshoot and system instability. Moreover, the model characteristics change dynamically and drive the system to different operation points. Therefore, an online adaptive gain scheduling PI is necessary for providing FCR due to the system's nonlinearity and the varying operational conditions. When providing FCR, the adaptive proportional and integral gains should be significant enough to respond quickly to the changes in the setpoint (when the error is significant). Then, after the power reference changes in reaction to the grid frequency (when the steady-state approaches), the proportional gain can decrease enough to ensure the system stability and avoid excessive overshoots, which negatively impact the mechanical loads. The following continuous transfer function can describe the PID controller:

$$G_c(s) = K_p\left(1 + \frac{1}{T_i s} + T_d s\right) \tag{11}$$

where K_p is a proportional gain. T_i and T_d are are the integral and derivative time constants. The PI controller can also be defined in discrete time as follows:

$$u(k) = u(k-1) + K_p \Delta e(k) + K_i e(k) \tag{12}$$

The control signal $u(k)$ is determined by knowing the error $e(k)$ between the reference signal and the output of the plant, the change of error that discretely specified as $\Delta e(k) = e(k) - e(k-1)$, and K_p and K_i represent the proportional and integral gains respectively. Although the derivative gain is not considered in this article due to high-frequency measurement noise, it has been calculated since it is required to obtain the integral gain. As shown in Figure 3, the fuzzy inference system has two inputs ($e(k)$,$\Delta e(k)$) and two outputs (K_{pp},K_{dp}) that are within the predefined ranges $[K_{p,\min}, K_{p,\max}]$ and $[K_{d,\min}, K_{d,\max}]$ respectively. The fuzzy outputs are calculated using the normalization method, given in [39], as follows:

$$K_{pp} = (K_p - K_{p,\min})/(K_{p,\max} - K_{p,\min}) \tag{13}$$

$$K_{dp} = (K_d - K_{d,\min})/(K_{d,\max} - K_{d,\min}) \tag{14}$$

where K_{pp} and K_{dp} are defined based on the fuzzy rules. These are defined in the form of IF-THEN, introduced by [39], for gain scheduling, and can be formulated as follows:

$$\text{If} \quad \begin{matrix} e \text{ is } A_i \\ \text{and} \\ \Delta e \text{ is } B_i \end{matrix}, \quad \text{Then} \quad \begin{matrix} K_{pp} \text{ is } C_i, \\ k_{dp} \text{ is } D_i, \\ \text{and} \\ \alpha = \alpha_i \end{matrix} \tag{15}$$

where A_i, B_i, C_i and D_i are fuzzy sets and α_i is a constant. The membership functions (MF) of these fuzzy sets for $e(k)$ and $\Delta e(k)$ are shown in Figure 7.a. Trapezoidal membership functions are used for (NB) and (PB), and Gaussian membership functions with the means of (-0.67,-0.33,0,0.33,0.67) and the same standard deviation of 0.14 are used for (NM, NS, ZO, PS, and PM). The grade of the membership function μ for these linguistic levels are defined as follows:

$$\begin{cases} \mu_{\text{NB}}(x) = \begin{cases} 0, & x > -0.7 \\ \frac{0.97+x}{0.27}, & -0.97 \leqslant x \leqslant -0.7 \\ 1, & x < -0.97 \end{cases} \\ \mu_{\text{PB}}(x) = \begin{cases} 0, & x < 0.7 \\ \frac{x-0.97}{0.27}, & 0.7 \leqslant x \leqslant 0.97 \\ 1, & x < 0.97 \end{cases} \end{cases} \tag{16}$$

$$\begin{cases} \mu_{\text{NM}}(x) = e^{-\frac{(x+0.67)^2}{0.04}}, & x \in \mathbb{R} \\ \mu_{\text{NS}}(x) = e^{-\frac{(x+0.33)^2}{0.04}}, & x \in \mathbb{R} \\ \mu_{\text{ZO}}(x) = e^{-\frac{x^2}{0.04}}, & x \in \mathbb{R} \\ \mu_{\text{PS}}(x) = e^{-\frac{(x-0.33)^2}{0.04}}, & x \in \mathbb{R} \\ \mu_{\text{PM}}(x) = e^{-\frac{(x-0.67)^2}{0.04}}, & x \in \mathbb{R} \end{cases} \tag{17}$$

The fuzzy sets C_i and D_i can be specified as either Big or Small by combining two Gaussian membership functions (gauss2mf in Matlab), also known as the two-sided Gaussian composite membership function, which is shown in Figure 7. The grade of these membership functions are expressed as follows:

$$\mu_{\text{Small}}(x) = \mu_{\text{Small-Left}}(x) * \mu_{\text{Small-Right}}(x)$$
$$\begin{cases} \mu_{\text{Small-Left}}(x) = e^{-\frac{(x+0.195)^2}{0.135}}, & x \leqslant -0.195 \\ \mu_{\text{Small-Right}}(x) = 1 - e^{-\frac{(x-0.195)^2}{0.135}}, & x \leqslant 0.195 \end{cases} \tag{18}$$

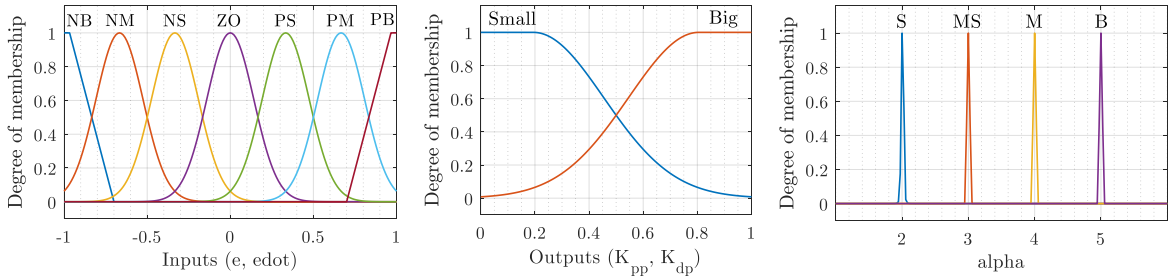

a. Membership function for error and error derivative, for K_{pp} and K_{dp}, and Singleton membership functions for α (left to right).

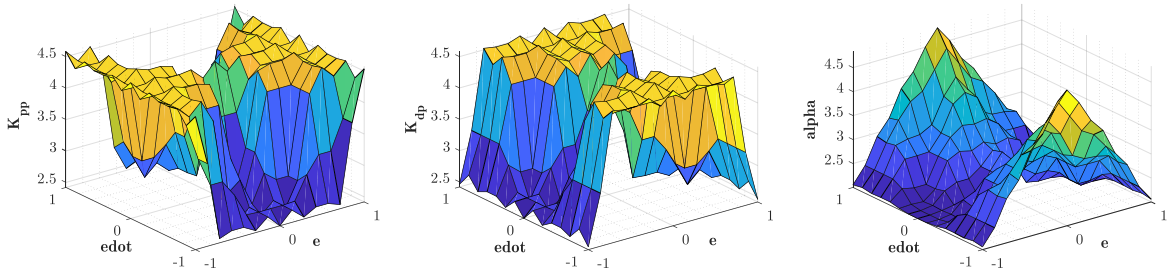

b. Surface view of the fuzzy rules

Figure 7: Fuzzy parameters.

$$\mu_{\text{Big}}(x) = \mu_{\text{Big-Left}}(x) * \mu_{\text{Big-Right}}(x)$$
$$\begin{cases} \mu_{\text{Big-Left}}(x) = e^{-\frac{(x-0.8)^2}{0.135}}, & x \leqslant 0.8 \\ \mu_{\text{Big-Right}}(x) = 1 - e^{-\frac{(x-1.195)^2}{0.135}}, & x \leqslant 1.195 \end{cases} \tag{19}$$

The proportional, derivative, and integral gains are given in (20), (21), and (22) and are determined using the method described in [39], which is based on the Ziegler-Nichols tuning technique.

$$K_p = K_{pp}(K_{p,\max} - K_{p,\min}) + K_{p,\min} \tag{20}$$

$$K_d = K_{dp}(K_{d,\max} - K_{d,\min}) + K_{d,\min} \tag{21}$$

$$K_i = \frac{{K_p}^2}{\alpha K_d} \quad \left(\alpha = \frac{T_i}{T_d}\right) \tag{22}$$

Relying on large-scale practices, the ranges of K_p and K_d are given as:

$$\begin{aligned} K_{p,\min} &= 0.32K_u \quad , \quad K_{p,\max} = 0.6K_u \\ K_{d,\min} &= 0.32K_uT_u \quad , \quad K_{d,\max} = 0.6K_uT_u \end{aligned} \tag{23}$$

where K_u and T_u are the gain and the period of oscillation that are measured when the stability limit is reached under ultimate P-control, and the controller output would oscillate with a constant amplitude.

The values of K_u and T_u are estimated in uniform wind conditions. The gains for the pitch and generator-torque controller are set as 8.00 and 4.50, respectively. For the pitch controller, 10.67 and 5.06 are taken as oscillation periods. Note that α is a constant described by the singleton membership function and has an integer value in the range from 2 to 5 [39].

Figure 3 shows the implementation of the proposed fuzzy controller. Based on the values of the error and the change in error inputs of the pitch and electrical power, the fuzzy inference system determines the values of the proportional and integral gains. The output of the speed controller is the current reference of the generator. The proposed nonlinear adaptive fuzzy-PI gains change continuously to optimally track the reference signals, which vary rapidly due to the wind speed and grid frequency changes.

4. Simulation results

4.1. Control performance

In this section, the performance of the adaptive power reserve provision is evaluated. It also compares the adaptive gain scheduled fuzzy-PI with the baseline controller under the fixed and percentage reserve mode strategies. The simulations have been carried out in partial and full load regions under turbulent wind conditions to challenge the robustness of the proposed controller. The wind speed profile is generated based on the Von Karman model, using the scaling parameter from the standard IEC 61400-1, edition 3 [40]. Furthermore, a grid frequency deviation profile provided by the Belgian transmission system operator (Elia) [41] is used, which activates upward and downward regulations and lets the WT power reserve be adjusted based on the proposed method in 3.

4.1.1. Partial load region

For the simulations in the partial load region, the WT is exposed to an 8 m/s mean wind speed with 10% Turbulence Intensity (TI). Figure 8.a shows the activation of the power reserve in the partial load region. The proposed controller is able to track the power reference signal under both reserve strategies and activate FCR with optimal deloading reserve.

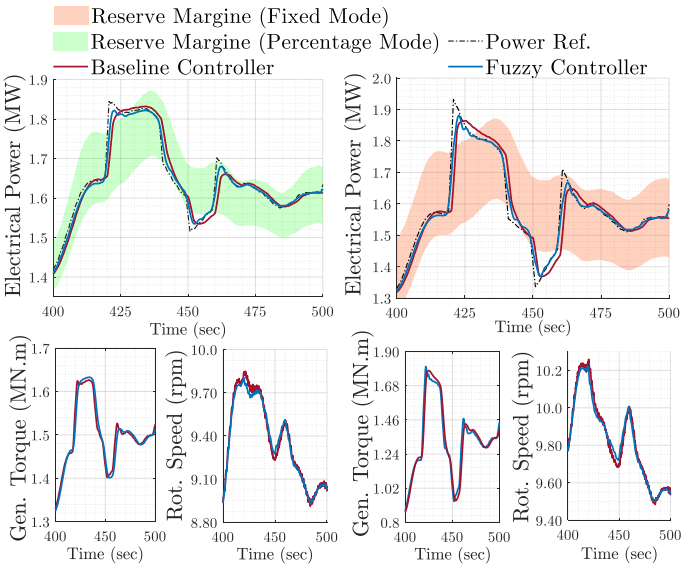

a. Performance of the proposed controller in power reference tracking and controlling generator torque and rotational speed.

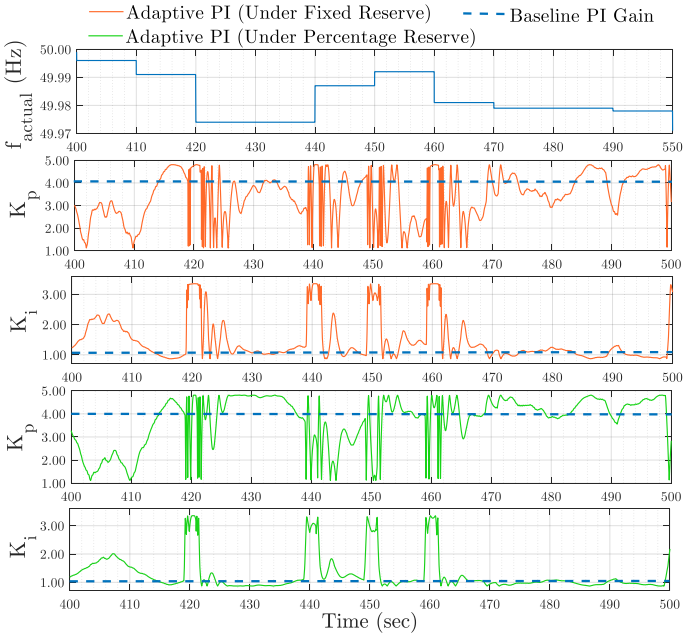

b. Adaptive fuzzy-PI gains (generator torque) versus baseline gains.

Figure 8: Activation of FCR in below-rated wind speed.

The simulation time is considered 550s to better compare the controllers. The Root Mean Square Error (RMSE) of the electrical power is calculated is calculated as a performance criterion. For the baseline controller under the fixed mode strategy and percentage mode strategy, the RMSE is 50.30 and 32.53 kW, respectively. At the same time, this parameter is reduced to 21.08 and 14.18 kW, respectively, by using the fuzzy-PI controller. As the main control input, the generator torque and the rotational speed are monitored for all the abovementioned cases. The proposed controller has a fast and adequate response while giving smoother rotational speed with small oscillation damping. In the simulation, the estimated power reserve is adapted to a maximum of 5% of the available wind power for both strategies. However, due to the inertia of the rotating mass, it can be seen around the time of 425s that the electrical power for a short duration can react up to 7.5% of the total power.

Moreover, Figure 8.b shows the adaptive proportional and integral gains of the generator-torque controller delivered by the fuzzy algorithm for a simulation of 100s (between 400s to 500s) following both reserves strategies and the turbulent wind condition. Figure 8.b depicts that when the grid frequency changes, the fuzzy proportional and integral gains are increased adaptively to reach and recompense the new operating point that has been changed due to the new power reference set point provided by the supplementary control loop. The proposed controller's adaptiveness feature would let the generator torque change adequately and fast without causing the rotor to overspeed.

4.1.2. Full load region

For wind speeds above the rated value, a derating control strategy is implemented in which the turbine will produce maximum power up to the desired power setpoint. In these simulations, an absolute power setpoint (maximum 95% of the rated power) is estimated to have a marginal reserve of maximum 250 kW for tracking the power signal, which proportionally corresponds to grid frequency changes. When the speed reaches the rated value, both percentage and reserve strategies can easily switch to the derating mode due to the constant rotational speed control. Figure 9.a illustrates the WT power reference tracking performance of the baseline and proposed fuzzy-PI controller in the above-rated wind speed, responding to the grid frequency profile that is already shown in Figure 6. The RMSE of the baseline controller is 25.93 kW, and this value is reduced to 20.58 kW when applying adaptive fuzzy-PI, which confirms that the proposed controller improves the control performance. Moreover, Figure 9.b depicts the pitch and generator torque behavior along with an improvement in rotor speed regulation in the case of employing the adaptive fuzzy-PI. The calculated RMSEs for the rotational speed under the proposed and baseline control strategies are 0.049 rpm and 0.08 rpm, respectively. The aerodynamic power sensitivity to the collective blade pitch angle, $\delta P/\delta\theta$, is an aerodynamic property of the rotor that depends on the wind speed, rotor speed, and blade-pitch angle. This study calculates pitch sensitivity based on a linearization analysis in FAST with AeroDyn for the NREL offshore 5MW WT baseline. The gain schedule PI as a baseline pitch controller is developed as suggested in [25]. The drivetrain gain and the negative damping from the generator-torque controller can be neglected for choosing appropriate PI gains. Therefore, the PI gains are calculated by knowing the recommended response characteristics along with the gain-correction factor. However, in the proposed fuzzy approach, no pitch sensitivity is included. Instead, an improved adaptation of control gains is offered that only considers the speed tracking error and the rate of this error. The torque control system will be involved in FCR provision in all operating regions. The power reference in the above-rated wind speed will be calculated through the supplementary

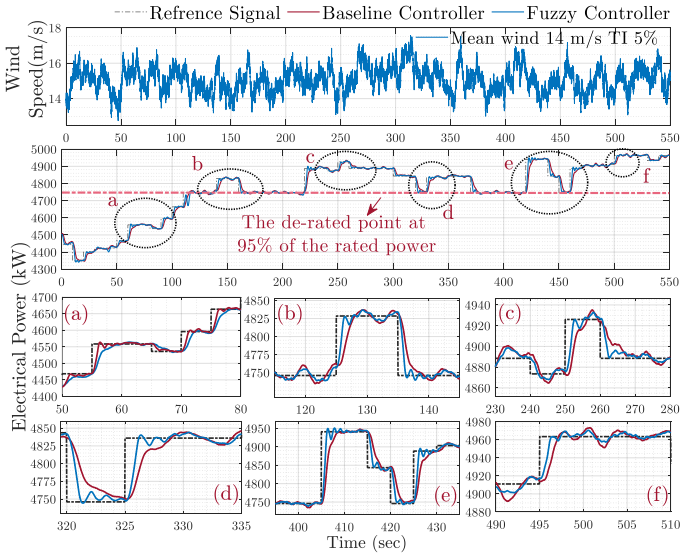

a. Power reference tracking of the proposed control system.

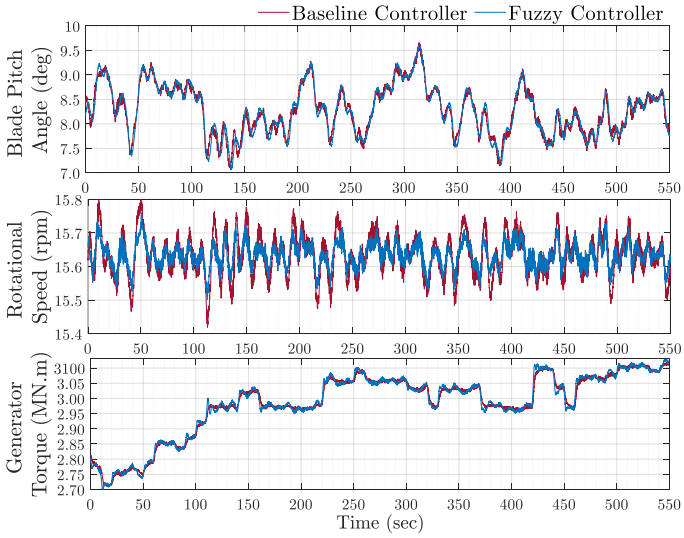

b. Performance of the pitch and generator torque and rotational speed of the proposed control system.

Figure 9: b. Activation of FCR in above-rated wind speed.

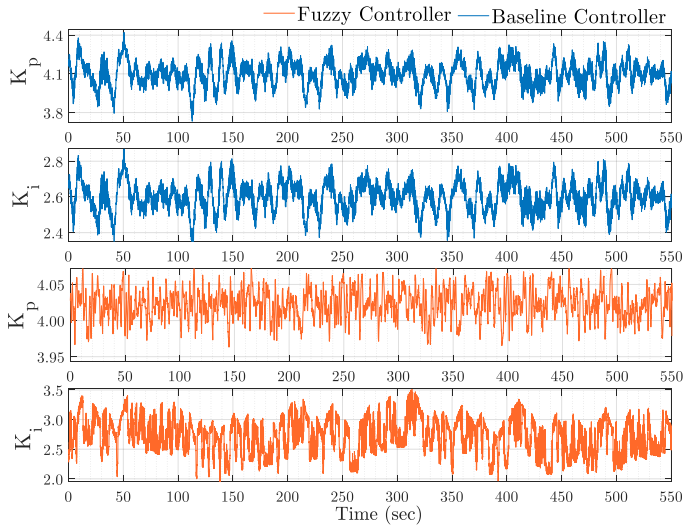

a. Pitch control system, adaptive fuzzy-PI gains versus baseline gains.

b. Generator torque, adaptive fuzzy-PI gains versus baseline gains.

Figure 10: Baseline and fuzzy controller gains in above-rated wind speed.

control loop given in section 3. However, the de-loaded power reference P_{dl} is fixed to a maximum derated margin at $0.05P_{rated}$, where P_{rated} is the nominal power at the rated wind speed. Figure 10 shows the PI gains of the pitch and torque controller of the fuzzy and baseline designs in responding to the grid frequency changes. The pitch controller's proportional and integral gains in the fuzzy approach are changing rapidly to offer a greater controlling and damping effect. On the other hand, the proportional and integral gains of the torque controller in the fuzzy approach, instead of fixed values in the baseline approach, are adaptively reacting to the varying electrical power setpoint, which respond to the grid frequency changes for providing FCR. When the power setpoint changes at the transient moment, the value of the proportional gain should become reasonably big, and the integral gain should be kept as small as possible to prevent an overshoot. When the steady-state approaches, the value of the proportional gain should decrease, and the value of the integral gain should increase to prevent further overshoots and oscillations. These conditions are well consolidated in the proposed fuzzy-based approach. Based on the simulation results that are reflected in Figures 9 and 10, the fuzzy-PI design has demonstrated better tracking and control performance compared to the baseline PI scheme.

4.2. *Analysis of mechanical load*

4.2.1. *Partial load region*

This subsection studies the effect of the proposed approach on the WT's mechanical load for each power reserve strategy. The root mean square (RMS) values are then calculated during the last 400s of the entire simulation. Since some mechanical loads would still be affected by the startup condition, the first 150s period is not considered in calculations. The blade root out-of-plane, tower base fore-aft, and tower base side-to-side bending moments for normal operation at MPPT and two

reserve strategies are illustrated in Figure 11.a. A remarkable increase in the amplitude of the blade root out-of-plane and tower base fore-aft bending moments are visible due to the cyclic loading, which will grow with increasing the rotor speed. In contrast, the amplitude of the tower base side-to-side bending moments is decreased. This result is expected because the side-to-side tower base bending moment depends on the torque moment caused by the roll motions at the top of the tower. In both strategies, the thrust force, responsible for the fore-aft tower base bending moment, is increased while the torque moment is decreased. This analysis should also explain the excessive mechanical loads in the fixed reserve strategy, which maintains a larger reserve than the percentage reserve strategy. Figure 11.b gives the RMS values of the other loading parameters in different control strategies. The blade root pitching, flapwise, and edgewise bending moments are also monitored in turbulent wind speed with a fixed pitch angle at zero degrees. The proposed control strategies have little effect on the blade edgewise moment. However, it can be detected that the fixed reserve strategy causes an increase in the blade root pitching and flapwise moments compared to the percentage reserve mode. Although both reserve strategies increase most of the affected mechanical loading parameters, applying the adaptive fuzzy-PI in below-rated wind speeds does not seem to add extra forces to the blade and tower base. The proposed control scheme slightly reduces the blade out-of-plane pitching and flapwise bending moments due to the smooth regulation of the rotor speed and the adaptive response of the generator torque to the varying power setpoint. Overall, the fuzzy-PI controller has superiority over the baseline PI controller in adjusting the electrical power and achieving the least RMS of the mechanical loads in the below-rated wind speed.

4.2.2. Full load region

As shown in Figure 9.b, applying the fuzzy-PI can effectively decrease the frequent action of the pitch actuator while providing improved power reference tracking and better rotor speed regulation compared to the baseline method. The lowered pitch servos and blade actions result in reduced mechanical loads. Figure 11.c compares the mechanical load parameters in nominal operation and derated mode under both control strategies. The proposed method alleviates the mechanical loads, especially the blade root edgewise and pitching moment, by effectively cooperating torque and pitch control in providing an active power regulation in the above-rated wind speed.

5. Conclusions

This article proposes an adaptive operational strategy for a WT providing Frequency Containment Reserve (FCR) considering grid frequency and wind speed stochastic behavior. An adaptive reserve margin is estimated based on a short-term prediction of the grid frequency. To be able to track the power reference signal, a real-time lookup table is employed in an FCR supplementary control loop to adjust the reserve margin and the control setpoints adaptively. The performance

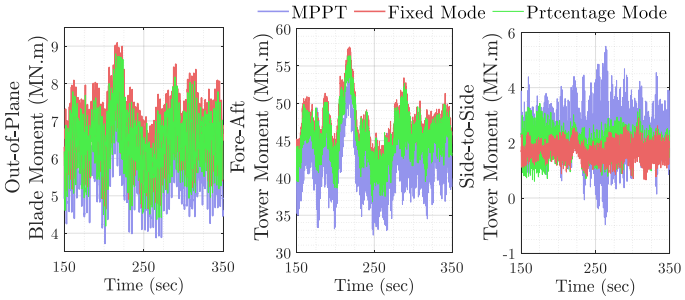

a. Time-series of mechanical loads in partial load region.

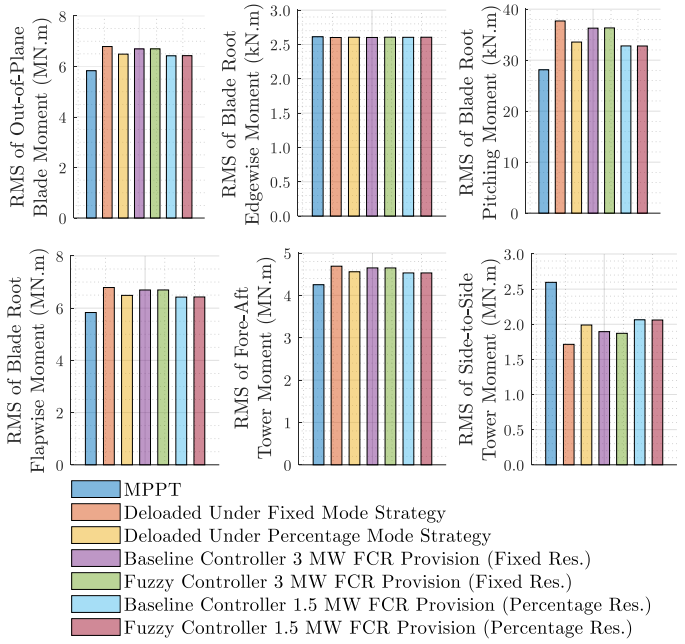

b. Applied mechanical loads for different control strategies in partial load region.

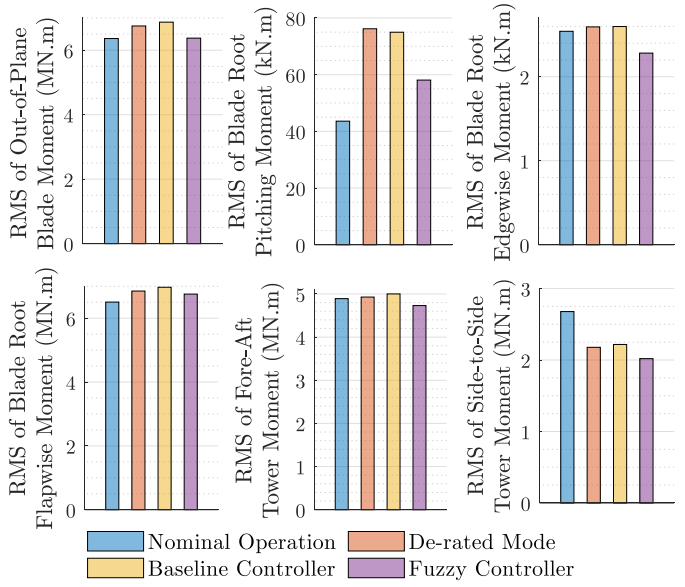

c. The WT mechanical loads for FCR provision in full load region.

Figure 11: Mechanical load analysis

of the suggested framework is investigated for two power reserve methods, i.e., fixed reserve and percentage reserve strategies. This study also addresses the gain scheduled fuzzy-PI design for adaptive and reliable control of a large offshore's operation (partial and full load regions) providing FCR in the presence of turbulent winds. The proposed controller is applied to the FAST simulator, which offers detailed nonlinear aero-hydro-servo-elastic simulation in the time domain for analyzing the effectiveness of pitch and torque control systems. The suggested adaptive reserve strategy performs well in terms of optimal and adequate response to the grid frequency changes. Moreover, the application of fuzzy-PI pitch and torque controllers for the proposed control structure is able to smoothen out electrical power fluctuations in an active power control mode and improve robust regulation of generator speed. No adverse impacts were found on mechanical loads that might be increased in particular conditions when providing the power reserve for the active power regulation. The simulation results indicate the superior performance of the adaptive fuzzy-PI in all operating regions and for both reserve modes. Besides the effectiveness and compatibility of the fuzzy-PI in terms of power reference tracking, it results in an optimal control action of pitch and torque in the presence of turbulent wind speed in below and above-rated wind conditions without risking the control system's stability. A general conclusion of this study suggests that the proposed operational strategy using adaptive gain scheduling fuzzy-PI is applicable and beneficial for FCR provision due to its inexpensive and computationally reasonable cost and capability to cover a broad range of operating conditions. Although providing power reserve increases some mechanical loads, this could be compensated by the adaptive and smooth performance of the proposed scheme, especially at above-rated wind speed and for fixed power reserve mode in below-rated wind speed. The proposed operational strategy can efficiently be integrated into a WT's existing pitch and torque control systems, enable them to provide FCR with optimal deloading margins and adaptively operate under different power reserve strategies.

Acknowledgment

This work was supported by the BEOWIND project funded by the Energy Transition Fund of the Belgian federal government managed by the FPS Economy.

References

[1] J. Shair, X. Xie, L. Wang, W. Liu, J. He, H. Liu, Overview of emerging subsynchronous oscillations in practical wind power systems, Renewable and Sustainable Energy Reviews 99 (2019) 159–168.

[2] GWEC (Global Wind Energy Council), GLOBAL WIND REPORT (2022).
URL https://gwec.net/global-wind-report-2022/

[3] T. Muneer, E. Jadraque Gago, S. Etxebarria Berrizbeitia, Wind energy and solar pv developments in the eu, in: The Coming of Age of Solar and Wind Power, Springer, 2022, pp. 139–177.

[4] ESO, Technical report on the events of 9 august 2019.
URL https://www.nationalgrideso.com/document/152346/download

[5] J. Đaković, M. Krpan, P. Ilak, T. Baškarad, I. Kuzle, Impact of wind capacity share, allocation of inertia and grid configuration on transient RoCoF: The case of the Croatian power system, International Journal of Electrical Power & Energy Systems 121 (2020) 106075.

[6] E. Rebello, D. Watson, M. Rodgers, Ancillary services from wind turbines: automatic generation control (AGC) from a single Type 4 turbine, Wind Energy Science 5 (1) (2020) 225–236.

[7] H. Algarvio, F. Lopes, A. Couto, A. Estanqueiro, Participation of wind power producers in day-ahead and balancing markets: An overview and a simulation-based study, Wiley Interdisciplinary Reviews: Energy and Environment 8 (5) (2019) e343.

[8] Z. Wu, W. Gao, T. Gao, W. Yan, H. Zhang, S. Yan, X. Wang, State-of-the-art review on frequency response of wind power plants in power systems, Journal of Modern Power Systems and Clean Energy 6 (1) (2018) 1–16.

[9] S. Li, W. Wang, X. Zhang, S. Qin, Y. Ying, A novel primary frequency regulation strategy of wind farm based on wind turbine health condition, IET Renewable Power Generation (2022).

[10] X. Bian, J. Zhang, Y. Ding, J. Zhao, Q. Zhou, S. Lin, Microgrid frequency regulation involving low-wind-speed wind turbine generators based on deep belief network, IET Generation, Transmission & Distribution 14 (11) (2020) 2046–2054.

[11] Q. Yao, Y. Hu, H. Deng, Z. Luo, J. Liu, Two-degree-of-freedom active power control of megawatt wind turbine considering fatigue load optimization, Renewable Energy 162 (2020) 2096–2112.

[12] X. Wang, Y. Wang, Y. Liu, Dynamic load frequency control for high-penetration wind power considering wind turbine fatigue load, International Journal of Electrical Power & Energy Systems 117 (2020) 105696.

[13] M. Cañas-Carretón, M. Carrión, Generation capacity expansion considering reserve provision by wind power units, IEEE Transactions on Power Systems 35 (6) (2020) 4564–4573.

[14] R. Prasad, N. P. Padhy, Synergistic frequency regulation control mechanism for dfig wind turbines with optimal pitch dynamics, IEEE Transactions on Power Systems 35 (4) (2020) 3181–3191.

[15] Z. Dong, Z. Li, Y. Dong, S. Jiang, Z. Ding, Fully-distributed deloading operation of dfig-based wind farm for load sharing, IEEE Transactions on Sustainable Energy 12 (1) (2020) 430–440.

[16] A. Fernández-Guillamón, G. Martínez-Lucas, Á. Molina-García, J. I. Sarasua, An Adaptive Control Scheme for Variable Speed Wind Turbines Providing Frequency Regulation in Isolated Power Systems with Thermal Generation, Energies 13 (13) (2020) 3369.

[17] A. Fernández-Guillamón, J. Villena-Lapaz, A. Vigueras-Rodríguez, T. García-Sánchez, Á. Molina-García, An adaptive frequency strategy for variable speed wind turbines: application to high wind integration into power systems, Energies 11 (6) (2018) 1436.

[18] M. Khamies, G. Magdy, S. Kamel, B. Khan, Optimal model predictive and linear quadratic gaussian control for frequency stability of power systems considering wind energy, IEEE Access 9 (2021) 116453–116474.

[19] N. Kayedpour, A. E. Samani, J. D. De Kooning, L. Vandevelde, G. Crevecoeur, Model predictive control with a cascaded hammerstein neural network of a wind turbine providing frequency containment reserve, IEEE Transactions on Energy Conversion 37 (1) (2021) 198–209.

[20] L. Pan, X. Wang, Variable pitch control on direct-driven PMSG for offshore wind turbine using Repetitive-TS fuzzy PID control, Renewable Energy 159 (2020) 221–237.

[21] B. Xu, Y. Yuan, H. Liu, P. Jiang, Z. Gao, X. Shen, X. Cai, A Pitch Angle Controller Based on Novel Fuzzy-PI Control for Wind Turbine Load Reduction, Energies 13 (22) (2020) 6086.

[22] T. Jeon, I. Paek, Design and Verification of the LQR Controller Based on Fuzzy Logic for Large Wind Turbine, Energies 14 (1) (2021) 230.

[23] Z. Civelek, Optimization of fuzzy logic (Takagi-Sugeno) blade pitch angle controller in wind turbines by genetic algorithm, Engineering Science and Technology, an International Journal 23 (1) (2020) 1–9.

[24] X. Zhang, Y. Chen, Y. Wang, X. Zha, S. Yue, X. Cheng, L. Gao, Deloading power coordinated distribution method for frequency regulation by wind farms considering wind speed differences, IEEE Access 7 (2019) 122573–122582.

[25] J. Jonkman, S. Butterfield, W. Musial, G. Scott, Definition of a 5-MW reference wind turbine for offshore system development, Tech. rep., National Renewable Energy Lab (NREL), Golden, CO (United States) (2009).

[26] J. M. Jonkman, M. L. Buhl, et al., FAST user's guide, Vol. 365, National Renewable Energy Laboratory Golden, CO, USA, 2005.

[27] P. J. Moriarty, A. C. Hansen, AeroDyn theory manual, Tech. rep., National Renewable Energy Lab., Golden, CO (US) (2005).

[28] J. D. M. De Kooning, J. Van de Vyver, B. Meersman, L. Vandevelde, Maximum efficiency current waveforms for a PMSM including iron losses and armature reaction, IEEE Transactions on Industry Applications 53 (4) (2017) 3336–3344.

[29] J. D. M. De Kooning, T. L. Vandoorn, J. Van de Vyver, B. Meersman, L. Vandevelde, Displacement of the maximum power point caused by losses in wind turbine systems, Renewable Energy 85 (2016) 273–280.

[30] J. Jonkman, S. Butterfield, W. Musial, G. Scott, Definition of a 5-MW Reference Wind Turbine for Offshore System Development, Technical Report (2 2009). doi:10.2172/947422.
URL https://www.osti.gov/biblio/947422

[31] J. Aho, L. Pao, P. Fleming, An active power control system for wind turbines capable of primary and secondary frequency control for supporting grid reliability, in: 51st AIAA Aerospace Sciences Meeting including the New Horizons Forum and Aerospace Exposition, 2013, p. 456.

[32] X. Ge, X. Zhu, Y. Fu, Y. Xu, L. Huang, Optimization of reserve with different time scales for wind-thermal power optimal scheduling considering dynamic deloading of wind turbines, IEEE Transactions on Sustainable Energy (2022).

[33] P. Fernández-Bustamante, O. Barambones, I. Calvo, C. Napole, M. Derbeli, Provision of frequency response from wind farms: A review, Energies 14 (20) (2021) 6689.

[34] J.-H. Urrea-Quintero, J. N. Fuhg, M. Marino, A. Fau, PI/PID controller stabilizing sets of uncertain nonlinear systems: an efficient surrogate model-based approach, Nonlinear Dynamics (2021) 1–23.

[35] K. Bedoud, M. Ali-rachedi, T. Bahi, R. Lakel, Adaptive fuzzy gain scheduling of PI controller for control of the wind energy conversion systems, Energy Procedia 74 (2015) 211–225.

[36] A. G. Aissaoui, A. Tahour, N. Essounbouli, F. Nollet, M. Abid, M. I. Chergui, A Fuzzy-PI control to extract an optimal power from wind turbine, Energy Conversion and Management 65 (2013) 688–696.

[37] G. Chen, T. T. Pham, N. Boustany, Introduction to fuzzy sets, fuzzy logic, and fuzzy control systems, Appl. Mech. Rev. 54 (6) (2001) B102–B103.

[38] Y.-M. Wang, Centroid defuzzification and the maximizing set and minimizing set ranking based on alpha level sets, Computers & Industrial Engineering 57 (1) (2009) 228–236.

[39] Z.-Y. Zhao, M. Tomizuka, S. Isaka, Fuzzy gain scheduling of PID controllers, IEEE Transactions on Systems, Man, and Cybernetics 23 (5) (1993) 1392–1398.

[40] B. J. Jonkman, Turbsim User's Guide: Version 1.50, Tech. rep., National Renewable Energy Lab.(NREL), Golden, CO (United States) (9 2009).

[41] www.elia.be, Belgian TSO providing transparency on grid data.
URL https://www.elia.be/en/grid-data